Understanding the Enzymatic Activity of 4-Oxalocrotonate Tautomerase and Its Mutant Analogues: A Computational Study

Tell Tuttle,*,† Ehud Keinan,‡,§ and Walter Thiel*,†

Max-Planck-Institut für Kohlenforschung, D-45470 Mülheim an der Ruhr, Germany, Department of Chemistry and Institute of Catalysis Science and Technology, Technion—Israel Institute of Technology, Technion City, Haifa 32000, Israel, Department of Molecular Biology and The Skaggs Institute of Chemical Biology, The Scripps Research Institute, 10550 North Torrey Pines Road, La Jolla, California 92037

Received: June 6, 2006; In Final Form: August 7, 2006

The effect of replacing arginine residues (Arg) with citrulline residues (Cit) in the binding site of 4-oxalocrotonate tautomerase (4-OT) was investigated with force field molecular dynamics and hybrid quantum mechanics/molecular mechanics studies. It is found that the Arg61Cit mutation has only minor effects on the k_{cat} and K_M values determined experimentally because of the flexibility of this residue. The decrease in k_{cat} and increase in K_M for the Arg11Cit and Arg39Cit mutations are due to the disruption of the binding site, which arises from repulsive interactions with neighboring residues. The results of this investigation shed new light on the effects of mutations in the binding site of 4-OT and consequently on how the enzyme binds the active substrate.

Introduction

The chemical mutation of highly active enzymes provides a powerful method for creating enzymes with new catalytic abilities, such as wider operational ranges (e.g., pH levels), enhanced or altered stereospecificity, and even selectivity to a greater (or novel) class of compounds.[1−4] These designer enzymes can be tailored to specific functions and as such have an important role to play in the developing field of biotechnology. The means by which such enzymes are created can be classified into two distinct groups: (1) directed evolution,[5−8] enzyme libraries with minor modifications are consecutively screened to find the optimum mutation scheme; (2) rational design,[3,4,9,10] specific residues within the active site are altered to produce the desired changes in the activity of the enzyme. In addition to the desired changes in catalytic activity, the latter approach may lead to a better understanding of the catalytic mechanism.

The process of rational design requires knowledge of the residues that compose the active site as well as their spatial arrangement. Consequently, this approach is most efficiently implemented when a three-dimensional structure of the enzyme is available. From this structure, residues are selected for the tuning of the catalytic activity. This strategy rests on two main assumptions: (1) the active site, in solution, with the substrate bound, is structurally close to that obtained from the X-ray study; (2) the mutation of residues does not significantly distort the active site structure.

4-Oxalocrotonate tautomerase (4-OT) is an enzyme that is produced by *Pseudomonas putida* mt-2 (a soil bacterium) and is active in a metabolic degradation pathway to convert aromatic hydrocarbons to energy.[11,12] The enzyme is formed as a trimer of dimers, where each monomer unit is 62 amino acids in length (Figure 1). The highly structured nature of the enzyme and the relatively short length of each subunit make it amenable to total chemical synthesis, and as such it has been the focus of several chemical mutation studies.[13−15]

The active sites of 4-OT (one per monomer) are positioned at the junction between dimers (Figure 1b), such that the substrate may be contacted by up to 3 separate monomers.[16] The substrate specific to 4-OT is 2-oxo-4*E*-hexendioate (**S**, Scheme 1). Once bound, the enzyme catalyzes the isomerization reaction resulting in 2-oxo-3*E*-hexendioate (**S′**). Experimentally, the isomerization reaction, when catalyzed by 4-OT, is extremely facile and proceeds with a maximum barrier of ca. 13 kcal/mol[15,17] (estimated from reported k_{cat} values using transition state theory). Through the use of data provided by Keinan et al.,[15] the proficiency[18] of the catalyst (i.e., $(k_{cat}/K_M)/k_{uncat}$) is $4.6 \times 10^9\ M^{-1}$. The high proficiency implies that the enzyme operates via covalent catalysis.[19]

Previous experimental[17,20−22] and theoretical studies[23] have confirmed the covalent role of 4-OT in catalyzing the isomerization of **S** to **S′**. The terminal proline residue (Pro1) was identified in these studies to act as a general base ($pK_a \approx 6.4$ in the hydrophobic active site) in transferring the proton from C3 to C5. (For atom numbering see Scheme 1.) In addition to the direct covalent role of Pro1, three arginine residues were identified crystallographically[16] that may play a role in the catalysis (Scheme 2). However the possibility of one of these residues acting as a general acid in an "acid−base catalysis" scenario has been excluded based on the experimentally determined pK_a values of the three arginine residues.[24]

The arrangement of the arginine residues around the inhibitor suggests their involvement in binding the substrate. However, whether the residues are able to provide additional stabilization for the TS complex through charge stabilization (as indicated in the mutation study by Keinan[15]) or whether their role is simply to anchor the substrate (as indicated in the mutation study by Whitman[17]) is unclear. Of particular interest is the work of the Keinan group where the arginine residues in the active site

* Authors to whom correspondence should be addressed. E-mail: tell@mpi-muelheim.mpg.de (T.T.); thiel@mpi-muelheim.mpg.de (W. T.).
† Max-Planck-Institut für Kohlenforschung.
‡ Technion—Israel Institute of Technology.
§ The Scripps Research Institute.

10.1021/jp0634858 CCC: $33.50
Published on Web 09/13/2006

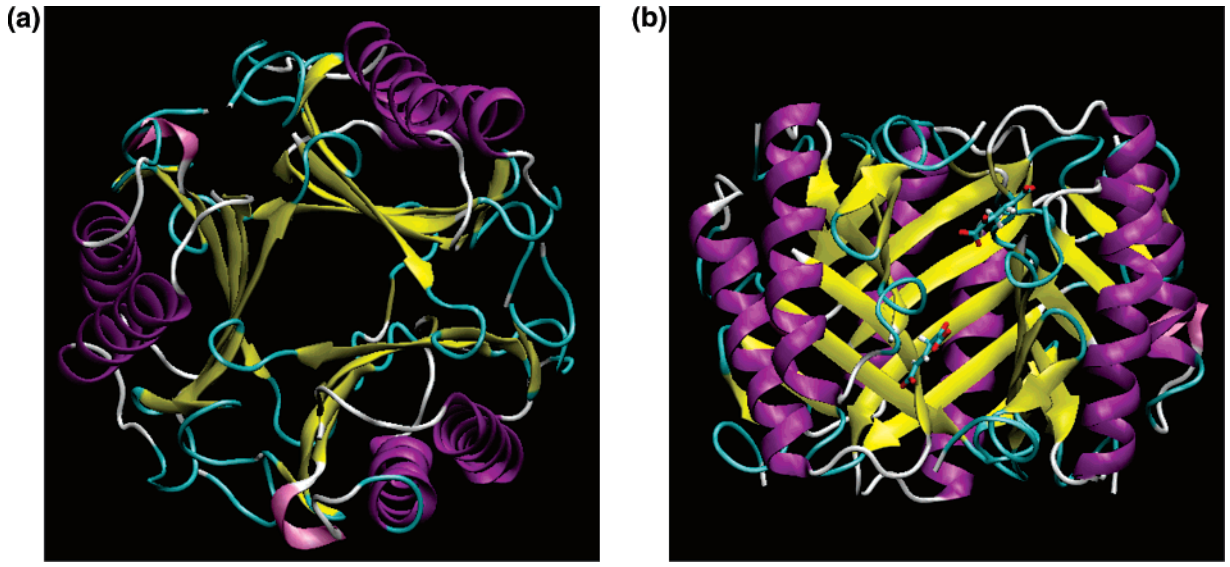

Figure 1. 4-Oxalocrotonate tautomerase. (a) Top view of enzyme showing the trimeric structure. (b) Binding sites of substrates (stick representation) are at the junction of two dimers.

SCHEME 1: Atom Numbering of the Substrate (S) and Resulting Isomerization Product (S′) Used in This Work

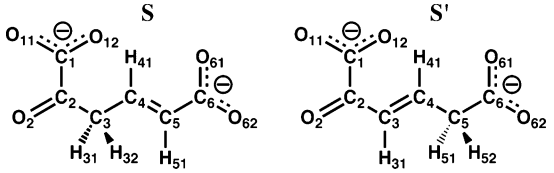

SCHEME 2: Schematic Representation of the Orientation of S in the Active Site of 4-OT[a]

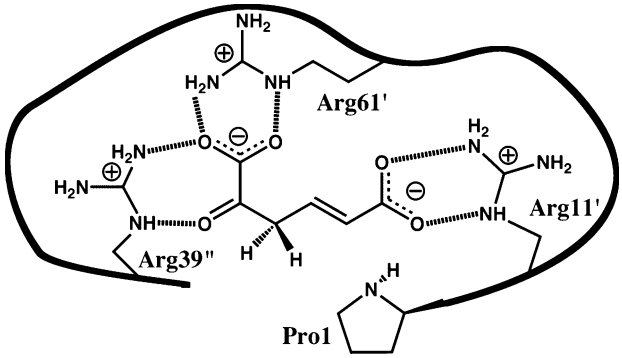

[a] Primed and double-primed notation indicates different monomer chains of the enzyme.[16]

SCHEME 3: Mutation from Arginine to Citrulline Replaces a Hydrogen-Bond Donor by a Hydrogen-Bond Acceptor

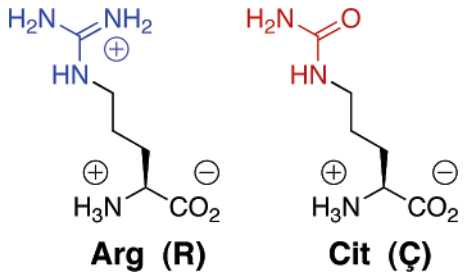

were replaced by the noncoded amino acid citrulline (Cit, Ç). Citrulline (Scheme 3) is a neutral isostere of arginine, and its use was proposed to elucidate a distinction between electrostatic and steric effects in the observed changes in k_{cat}/K_M. However, the mutation of Arg → Cit exchanges a hydrogen-bond donor group for a hydrogen-bond acceptor, and the effect of this exchange on the structure of the active site is unclear.

In the current work we investigate, computationally, the effects of the Arg → Cit mutation on the structure of one of the active sites in the enzyme with the substrate present. Experimentally this type of information is inaccessible due to the inability to obtain a crystal with the substrate bound to the enzyme, and thus the active site is generally assumed to maintain the steric properties of the wild-type enzyme after the mutation. The validity of this assumption is assessed using a combination of force-field-based molecular dynamics (MD) and hybrid quantum mechanical/molecular mechanical (QM/MM) studies as explained in the following section.

Computational Methods

System Preparation: Classical Simulations. The structure of the enzyme, taken from the Protein Data Bank (PDB code 1BJP), is an inactive form and contains the covalently linked inhibitor 2-oxo-3-pentynoate.[16,25] Although there are several deposited structures of 4-OT in the Protein Data Bank, the deactivated form was chosen as this is expected to be the closest representation of the structure once the substrate is bound. The PDB file contains five segments (A−E) corresponding to two dimers and one monomer of *H*32 symmetry. The *H*32 symmetry is not implemented in Sybyl[26] (the program package that we used to generate a complete set of coordinates for 4-OT); therefore the trigonal space group (*P*2*m*1), which restores the two dimers to hexamers, was used. Noncrystallographic restraints were applied in the generation of the original PDB coordinates, which implies that dimer pairs were constrained to be identical. Thus, we used the hexamer generated from segments A and B to study the system.

The program Reduce,[27,28] which accounts for the generation of hydrogen-bond networks and potential steric clashes, was used to add hydrogen atoms and to adjust the orientations of the Asn, Gln, and His side chains where necessary. All changes made to the original PDB structure, and the orientations of the His residues defined by Reduce were checked by visual inspection. (The complete list of changes made to the structure is provided in the Supporting Information.) The protonation

SCHEME 4: Substitution Scheme and Nomenclature (Blue) for Labeling the Wild-Type 4-OT and Mutants[15]

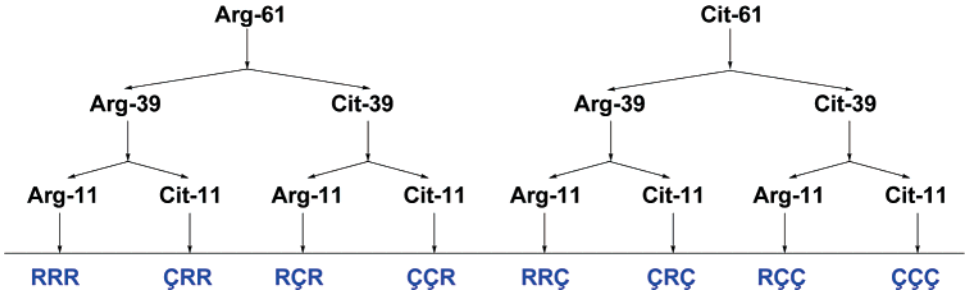

states of ionizable residues were assigned based on a previous theoretical study[29] and cross-checked with the empirical pK_a prediction program, PROPKA.[30]

The coordinates for the wild-type 4-OT were then modified to substitute the selected arginine residues with citrulline to create the mutant systems. The sequential substitution of the arginine residues results in seven chemically different mutants (Scheme 4). However, the placement of the side-chain carbonyl group of Cit is ambiguous due to a potential repulsion with neighboring residues. Thus, 27 different conformational variants were created to cover all possibilities and to avoid any bias through the chosen orientation of the side chain.

All fully classical calculations (including hydration of the system, MM minimizations, and MD simulations) were carried out with the CHARMM program.[31−33] The wild-type 4-OT and mutant systems contain special residues that are not provided in the standard CHARMM force fields[34−36] used in this work. Thus CHARMM parameters and topologies were developed for the neutral terminal proline residue, the citrulline residue, and **S**, using the CHARMM procedure[34,36] for the calculation of partial charges to obtain a description of the nonbonding interactions that is consistent with the remainder of the force field.[37] Parameters describing intramolecular interactions (e.g., stretching, bending, etc.) were generated by analogy with existing CHARMM residues. (Details of the parameter development are provided in the Supporting Information.)

The substrate molecules (**S**) were placed in the active sites of the enzyme using the position of the covalently linked inhibitors for an initial alignment. The 6-carboxylate group (see Scheme 1 for numbering), which is not present in the inhibitor, was positioned such that it could interact with Arg11 through hydrogen bonding (in the orientation indicated in Scheme 2) as has been proposed from the experimental mutation studies.[15,17] After deletion of the inhibitors the substrate molecules were relaxed through an MM energy minimization, while all other atoms were kept fixed. From this structure, one substrate conformation (**S1**) was selected as the focus for the subsequent calculations, and the system was centered on the C3 atom of this substrate.

The system was hydrated using the droplet model with a 30 Å sphere of equilibrated TIP3P water centered at the C3 atom of **S1**. All waters that overlapped[38] with the complex were deleted. All water molecules in the 30 Å sphere were geometry-optimized and subsequently subjected to an MD run for 100 ps at 300 K using Langevin dynamics. A stochastic boundary potential[39] was used to maintain the structure of the water sphere, while all nonwater atoms were frozen during both the geometry minimization and the equilibration period. We performed this hydration procedure five times, at which point the number of added water molecules remained approximately constant.

The nonwater residues containing atoms within 20 Å of the center of the system (C3 atom of **S1**) were defined as being in an active region. This active region, along with all TIP3P waters, underwent a 1 ns MD simulation at 300 K using Langevin dynamics. The boundary potential for the water molecules used in the hydration procedure was again employed. For full details of the parameter development, hydration procedures, geometry optimization, and MD simulations, refer to the Supporting Information.

QM/MM Setup. The QM/MM calculations were carried out in two stages: (a) an initial geometry optimization of the reactant at the AM1[40]/CHARMM level of theory; (b) final optimization of the minima at the (BLYP[41,42]/TZVPP[43])/CHARMM level of theory. The modular program package ChemShell[44,45] was used for all QM/MM calculations, where the QM energy and gradients were provided by MNDO99[46] (QM = AM1) or TURBOMOLE[47−51] (QM = BLYP). ChemShell's internal force field driver using the CHARMM parameter and topology data provided the MM energy and gradients. No electrostatic cutoffs were used, neither between the QM and the MM regions nor within the MM region alone. The QM density was electrostatically embedded into the MM environment by including the point charges from the MM atoms into the QM Hamiltonian. The boundary region was treated with the charge-shift scheme,[45,52] which provides a reliable treatment of the coupling between the QM and the MM zones.[53,54] The bonded and van der Waals interactions between the QM and the MM regions are handled at the MM level of theory, as described previously.[45]

The QM region contains the substrate (**S1**) and the terminal proline (**P1**) adjacent to **S1**, resulting in 30 QM atoms. The covalent bond across the QM/MM boundary is the C−N amide bond between Pro1 and Ile2; within the QM calculations the carbon atom is saturated with a hydrogen-link atom. The cut between the QM and MM regions coincides with the CHARMM charge-group definitions such that the QM and MM regions both have integer charges. For the QM/MM geometry optimizations a subset of the total system is optimized while the remainder of the atomic positions are frozen. The active subset for all optimizations was defined from the initial reactant complex geometry using a distance criterion, whereby any residue that contains an atom within 10.0 Å of *any* atom of **S1** is included in the active subset. The resulting active region contains ca. 1100 atoms (1114 for **RRR**), about one tenth of the total system size (ca. 13 500 atoms).

The QM/MM geometry optimizations were performed with HDLCOpt,[55] a linear scaling, microiterative algorithm which employs a set of hybrid delocalized coordinates, as implemented in ChemShell. The residues defined for this optimization procedure were taken as the standard residues defined for CHARMM (e.g., amino acids, waters, and substrate). Further details of the QM/MM setup and the partitioning of the active region for each mutant are provided in the Supporting Information.

TABLE 1: Hydrogen-Bond Descriptors of S1 in the RRR System[a]

interaction	$\bar{r}$	$\bar{\tau}$	$\bar{r}r_{-1}$	$\bar{\tau}_{-1}$	P
(**R11**)H−O61	1.75	99.3	2.96	1.1	0.99
(**R11**)H−O62	1.64	1001			1
(**R39**)H−O2	2.24	11.0	3.01	1.2	0.90
(**R39**)H−O11	1.78	332.3	2.96	1.0	0.99(7)
(**R61**)H−O11	1.89	67.7	3.02	1.89	0.98
(**R61**)H−O12	1.77	123.0	3.15	2.20	0.99
(**P1**)N−H3	2.64	2.27	3.00	2.15	0.52
(**P1**)N−C5			4.44	1001	

[a] See the text for definitions of symbols. Distances are given in angstroms. Times are given in picoseconds

Results and Discussion

The orientations of the substrate and the residues comprising the binding site of the wt-4-OT (**RRR**) are not unambiguously defined. The initial orientation that we have chosen for **S1** is in accord with the observation that Arg11 plays an important role in binding the substrate. However, as no experimental structures are available for the reactant complex, this is an assumed orientation, and we therefore performed a 1 ns MD simulation on the **RRR** complex to allow the binding site to equilibrate. The binding site orientation that we have employed involves the substrate interacting with the three arginine residues through strong hydrogen bonds and with the terminal proline through a weak (C)H···N hydrogen bond. Thus, the changes in the binding site structure during the simulation can be monitored by the trajectory of these hydrogen bonds. We consider a hydrogen bond (Y−H···X_{acc}) to be present if $R_{H-X_{acc}} \leq 2.8$ Å (X_{acc} = O or N). In addition we use several time-dependent descriptors for hydrogen bonds: $\bar{r}$, average length of hydrogen bond; $\bar{r}_{-1}$, average separation of atoms when $R_{H-X_{acc}} > 2.8$ Å; $\bar{\tau}$, average lifetime of hydrogen bond; $\bar{\tau}_{-1}$, average lifetime when $R_{H-X_{acc}} > 2.8$ Å; $P = N_{H-bond}/N_{tot}$, the fraction of snapshots involving a hydrogen bond for the atom pair. These descriptors provide direct information about the stability of the substrate in the binding site through the lifetime and strength (as a function of distance) of the respective hydrogen bonds during the simulation.

RRR: MD Simulation. In the wild-type enzyme, the binding between the 6-carboxylate group and **R11′** is stabilized by two strong hydrogen bonds. The hydrogen bond between O61 and **R11′** has an average length of 1.75 Å ($\bar{r}$, Table 1) and is present in the structure for more than 99% of the simulation (*P*, Table 1). The separation of the atoms beyond the threshold specified for the hydrogen-bond formation occurs intermittently ($\bar{\tau} = 99.3$ ps) and is rapidly reformed ($\bar{\tau}_{-1} = 1.1$ ps). The second hydrogen bond between **S1** (O62) and **R11′** is even stronger than the first ($\bar{r} = 1.64$ Å) and is retained throughout the entire simulation. These results show that the binding interaction between **S1** and **R11′** is strong and very likely to be present in the real system. Although this orientation differs from that used in a previous study,[23] we are confident that our orientation of the substrate in the binding site is consistent with the experimental evidence[2,15,17,24,56] of an interaction with **R11′** and that it is the preferred orientation as it yields a tight binding of the substrate.

Residue **R39″** has been identified in the experimental studies as being important for both binding of the substrate and catalytic activity.[2,15,17,24,56] The crystal structure used in constructing the **RRR** system (1BJP) clearly indicates an interaction between the carbonyl oxygen of the inhibitor and the H(N_ϵ) atom of **R39″**. In the MD simulation this interaction is retained with **S1** (O2), although it is weaker ($\bar{r} = 2.24$ Å) than the hydrogen bonds formed with the carboxylate oxygens, as expected. The decrease in the strength of the hydrogen bond is reflected in the greater average length, relative to the hydrogen bonds formed with carboxylate oxygen atoms, as well as the tendency of the hydrogen bond to break and reform at regular intervals ($\bar{\tau} = 11.0$, $\bar{\tau}_{-1} = 3.0$ ps). **R39″** also has a strong interaction ($\bar{r} = 1.78$ Å) with one of the 1-carboxylate oxygen atoms (O11) that is present for the majority of the simulation ($\bar{\tau} = 332.3$ ps).

The third arginine residue in the binding site (**R61′**) is the subject of much debate, regarding its role in substrate binding and catalysis. The mutation studies of Keinan show that the substitution of Cit for **R61′** has little effect on the catalytic activity or binding of the substrate.[15] Furthermore, alternative X-ray structures of 4-OT, without the inhibitor bound, do not have the **R61′** residue in the same position as in the case of the enzyme with the inhibitor bound.[57] As explained in the previous section, we have used the inhibitor-bound structure, which shows a strong interaction between the carboxylate group of the inhibitor and **R61′**. As seen in Figure 2, this interaction is present in our starting structure and remains throughout the simulation. The hydrogen bond between **R61′** and O11 is slightly longer than the other ionic hydrogen bonds calculated ($\bar{r} = 1.89$ Å) due to the competition between **R61′** and **R39″** for binding to this atom. This competition also results in occasional breaking and reforming of the hydrogen bond ($\bar{r}_{-1} = 3.0$ Å, $\bar{\tau}_{-1} = 1.9$ ps). However, the hydrogen bond is present for more than 98% of the simulation and clearly provides a stabilizing interaction for the binding of the substrate. The second hydrogen bond with **R61′** is again a strong ionic interaction ($\bar{r} = 1.77$ Å), and apart from some minor fluctuations ($\bar{\tau} = 123.0$, $\bar{\tau}_{-1} = 2.2$ ps) it remains consistently throughout the simulation. The tight binding between **R61′** and **S1** (as demonstrated by short $\bar{r}$) and the stability of these interactions (long $\bar{\tau}$) suggest that the chosen orientation of **R61′** is a legitimate and favorable positioning of the residue.

The interaction between **S1** and the neutral, terminal proline residue (**P1**) is much weaker ($\bar{r} = 2.64$ Å) than the strong, formal hydrogen bonds formed with the arginine residues. According to our definition ($R_{H-X_{acc}} \leq 2.8$ Å) the hydrogen bond appears in only 52% of the snapshots from the simulation. The weak nature of the interaction is also reflected in the average lifetime of the system when the hydrogen bond is present and when it is not ($\bar{\tau} = 2.3$, $\bar{\tau}_{-1} = 2.2$ ps), which indicates that the hydrogen bond is being broken and reformed on a regular basis. This is consistent with the nature of the donor group (C3) and the neutral acceptor atom (N). Despite the weak interaction, the substrate is clearly well positioned in the binding site for the proton transfer to occur. When the atom separation exceeds our definition for the hydrogen bond, the average separation is only 3.00 Å. Thus, although the interaction between **P1** and **S1** is weak, the orientation of the substrate in the active site allows the reaction partners to remain in close proximity.

The second step in the isomerization reaction involves the transfer of a proton from N1 of **P1** to the C5 atom of **S1**, and as such the relative positioning of the C5 atom to N1 is also monitored during the MD simulation (Figure 2). The (**P1**)N···C5 separation will most likely be strongly affected by the formation of the intermediate structure that involves the protonated proline. Nonetheless, the average separation of these atoms throughout the simulation is 4.44 Å, although there is a clear transition after ca. 400 ps to larger interatomic distances. This distance is still consistent with the involvement of the C5 atom in the proton transfer, once the intermediate is formed.

RRÇ: MD Simulation. Experimentally the Arg61Cit mutation has only a minor impact on the K_M and k_{cat} values.[15] This observation was taken to indicate that Arg61 plays only a minor

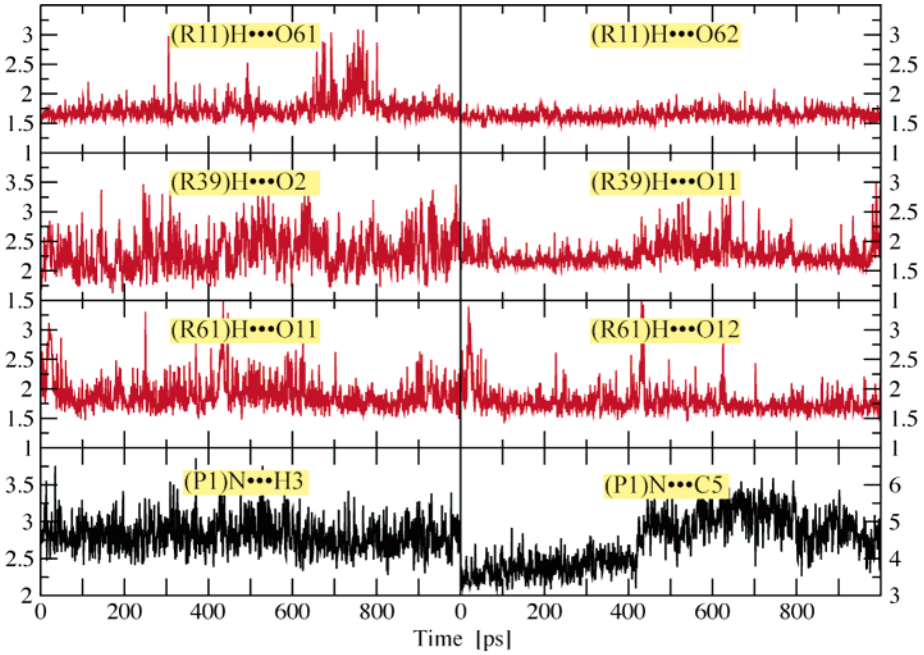

Figure 2. Trajectory of hydrogen bonds in the binding site for the **RRR** system.

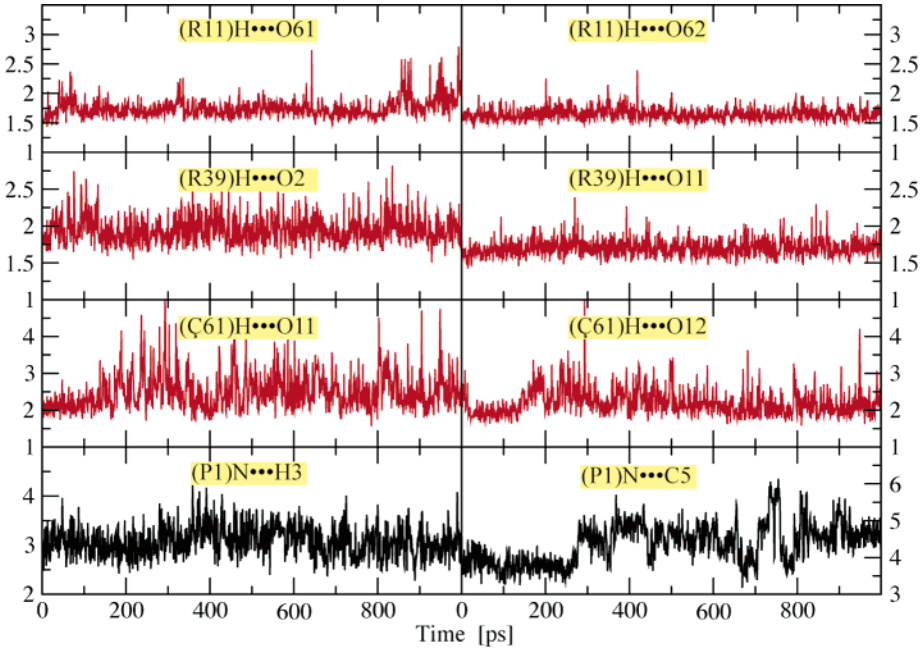

Figure 3. Trajectory of hydrogen bonds in the binding site for the **RRÇ** system.

role in substrate binding and catalysis. However, as discussed above, we find that for the wild-type enzyme **R61′** forms strong hydrogen bonds with the substrate ($\bar{r}$ = 1.89, 1.77 Å, Table 1) and thus stabilizes **S1** in the binding site. In the **RRÇ** mutant, the preferred orientation of the carbonyl oxygen atoms of the citrulline residue is not known a priori. Therefore, we performed MD simulations for all possible conformations and selected the system with the most stable binding site, based upon the number and strength of hydrogen bonds between the substrate and the selected residues. (Full details of the selection procedure are available in the Supporting Information.)

The analysis of the MD simulations of the possible **RRÇ** systems shows that the preferred orientation of the citrulline residue at position 61 involves the carbonyl oxygen atom (blue O atom in Scheme 3) pointing away from the substrate. This is consistent with the expected lone-pair repulsion that would result if the carbonyl oxygen atom of **Ç61′** is directed toward the 1-carboxylate group of **S1**. Moreover, residue 61 is on the surface of the enzyme and is relatively flexible, due to its proximity to the C-terminus of the monomer, as such it is free to adjust its position to create the most favorable binding site for the substrate. In Figure 3, it is evident that the hydrogen bonds formed between residue 61 and **S1** remain intact, although these are now weaker relative to **RRR**, which is consistent with the previously cationic arginine residue becoming neutral.

The changes in the relative strength of the hydrogen bonds are expressed in the hydrogen-bond descriptors, which also indicate a rotation in the binding site that leads to shorter **R39″**−**S1** interactions. The average hydrogen-bond length ($\bar{r}$) of the **Ç61′**−**S1** hydrogen bonds has increased from 1.89 and 1.77 Å to 2.28 and 2.14 Å, respectively (**RRR** vs **RRÇ**). In addition, the contact formed between the two residues is clearly less stable

TABLE 2: Hydrogen-Bond Descriptors of S1 in the RRÇ System

interaction	$\bar{r}$	$\bar{\tau}$	$\bar{r}_{-1}$	$\bar{\tau}_{-1}$	P
(**R11**)H−O61	1.75	993	2.80	1.0	0.99(9)
(**R11**)H−O62	1.65	1001			1
(**R39**)H−O2	1.95	835.0	2.85	1.0	0.99(9)
(**R39**)H−O11	1.70	1001			1
(**Ç61**)H−O11	2.28	6.1	3.24	1.89	0.77
(**Ç61**)H−O12	2.14	18.1	3.15	1.35	0.93
(**P1**)N−H3	2.67	1.52	3.19	5.68	0.21
(**P1**)N−C5			4.37	1001	

[a] See the text for definitions of symbols. Distances are given in angstroms. Times are given in picoseconds.

TABLE 3: Hydrogen-Bond Descriptors of S1 in the RÇR System[a]

interaction	$\bar{r}$	$\bar{\tau}$	$\bar{r}_{-1}$	$\bar{\tau}_{-1}$	P
(**R11**)H−O61	1.88	52.8	2.93	1.1	0.98
(**R11**)H−O62	1.66	1001			1
(**Ç39**)H−O2	2.27	8.1	3.32	3.4	0.70
(**Ç39**)H−O11	2.43	3.1	4.37	20.1	0.14
(**R61**)H−O11	2.29	3.1	3.06	2.9	0.54
(**R61**)H−O12	2.31	2.2	3.11	4.4	0.37
(**P1**)N−H3	2.65	1.8	3.08	3.9	0.31
(**P1**)N−C5			4.33	1001	

[a] See the text for definitions of symbols. Distances in are given in angstroms. Times are given in picoseconds.

as the average lifetime of the hydrogen bond ($\bar{\tau}$) is decreased by an order of magnitude. However, the overall binding of **S1** is not affected much by this decrease as there is a stronger interaction between the carbonyl O atom (O2) of **S1** and **R39″**, as compared with the **RRR** system ($\bar{r}$ = 1.95 Å and $\bar{r}$ = 2.24 Å, respectively**)**. The stronger interaction between **S1** and **R39″** has only a minor influence on the positioning of the proton for abstraction. The average length of the (**P1**)N···H3 hydrogen bond increases slightly from 2.64 to 2.67 Å. However, it is formed less often in the **RRÇ** system (P = 0.21), and the average separation when no hydrogen bond is present is increased to 3.19 Å. Nonetheless, the ability of the mutant to position the substrate in a manner similar to the wild-type enzyme is consistent with the minimal decrease in k_{cat} observed experimentally. Thus, we conclude that **R61′** does play a role in binding the substrate and that the Arg61Cit mutation affects the experimentally observed properties only slightly because of the flexibility of residue 61, which allows **Ç61′** to bind the substrate almost as efficiently as the original residue, **R61′**.

RÇR: MD Simulation. Experimentally, the mutation of **R39″** to citrulline was found to have a dramatic effect on the catalytic ability (k_{cat}) of the enzyme, although the observed changes to K_M were not significant.[15] The different effects on the binding ability of the enzyme and the catalytic activity were attributed to the ability of **R39″** to stabilize the intermediate of the reaction through electrostatic complementarity, which is removed in the Arg39Cit mutation. These conclusions were based on a static picture of the binding site, assuming that the Arg39Cit mutation does not affect the structure of the binding site. We performed an MD simulation on the **RÇR** mutant to test this assumption. As described in the **RRÇ** system, the orientation of **Ç39″** resulting in the strongest binding of the substrate was selected. (See the Supporting Information for results of all systems.)

The MD simulation of **RÇR** reveals a markedly different hydrogen-bond profile relative to the **RRR** system. Although the hydrogen bonds between **S1** and **R11′** remain strong ($\bar{r}$ = 1.88, 1.66 Å) and consistent (P = 0.98, 1) throughout the simulation, the interaction with residue 39 is clearly affected (Table 3). The hydrogen bond between the carbonyl O atom of **S1** and **Ç39″** persists through the first 500 ps of the simulation and fluctuates more in the latter half, although it is still present in the majority of cases (P = 0.70). The average length of this hydrogen bond is similar to the wild-type system, although its lifetime is reduced relative to **RRR** ($\bar{\tau}$ = 8.1 vs 11.0 ps, respectively) and the separation of the atoms when the interaction is lost ($\bar{r}_{-1}$**)** is also greater (**RÇR**, 3.32 Å; **RRR**, 3.01 Å). The hydrogen bond between the 1-carboxylate group of **S1** and **Ç39″** is much more strongly affected by the mutation. After the first ca. 150 ps, which are considered as an equilibration period, the bond is effectively broken (P = 0.14) with an average separation of the atoms of 4.37 Å (Table 3).

The interaction of the substrate with **R61′** is also changed by the Arg39Cit mutation. Despite maintaining electrostatic complementarity with the substrate, the interactions with **R61′** are weakened ($\bar{r}$ > 2.2 Å) and fluctuate more rapidly ($\bar{\tau}$ = 2−3 ps). Furthermore, the binding of the substrate by **Ç39″** and **R61′** appears to be coupled, as is evident in the trajectories of the hydrogen bonds during the 750−800 ps interval: The (**Ç39″**)H···O2 bond is broken, while the (**Ç39″**)H···O11 bond is formed and the hydrogen bonds between **R61** and the substrate are both strengthened. This cooperativity between the two residues is plausible because of their close proximity in the binding site and their ability to bind the same atoms of the substrate. (See the discussion of binding sites below for details.)

Despite the weakening of the hydrogen bonds between **S1** and the **Ç39″** and **R61′** residues, the ability of **RÇR** to bind the substrate is not significantly decreased as residues 61 and 39 are able to operate in concert to bind the 1-carboxylate end of **S1**. In the **RÇR** system, the positioning of the substrate relative to **P1** is similar to that in the **RRR** system. This indicates that there should be little difference in the ability of the enzyme to abstract the proton from **S1**; however, experimentally, there is a large change in the observed k_{cat} value for this mutant.[15]

ÇRR: MD Simulation. Experimentally, the Arg11Cit mutation resulted in a strong decrease in both the binding and the catalytic ability of the enzyme.[15] The lowered binding ability of the enzyme is caused by the loss of the two hydrogen bonds with residue 11, which exist in **RRR**. In the **ÇRR** system, the interaction with **Ç11′** is quickly lost (within 50 ps) during the MD simulation (Figure 5). The substitution of this residue results in a repulsive interaction with **S1** such that the average separations of the atoms are 8.32 and 7.40 Å ($\bar{r}_{-1}$, Table 4). This repulsive interaction remains throughout the MD simulation. This loss of the 6-carboxylate binding interactions is only partially compensated by the stronger hydrogen bonds with **R61′** and **R39″**: Both hydrogen bonds to **R61′** in the **ÇRR** system have an average bond length of <1.8 Å, and the hydrogen bond between O2 and **R39″** is shorter ($\bar{r}$ = 2.13 Å) than that in the **RRR** system.

As was observed in the **RÇR** system, the positioning of **S1**, relative to **P1**, is maintained in the **ÇRR** mutant. The hydrogen bond between H3 of **S1** and N of **P1** is present in 55% of the snapshots (P = 0.55, Table 4). This is somewhat surprising given the expected greater flexibility of the substrate to move around the binding site once the 6-carboxylate terminus is no longer anchored by residue 11. The electrostatic stabilization of the additional negative charge in the intermediate state is not strictly localized to the O2 atom; thus the complete loss of

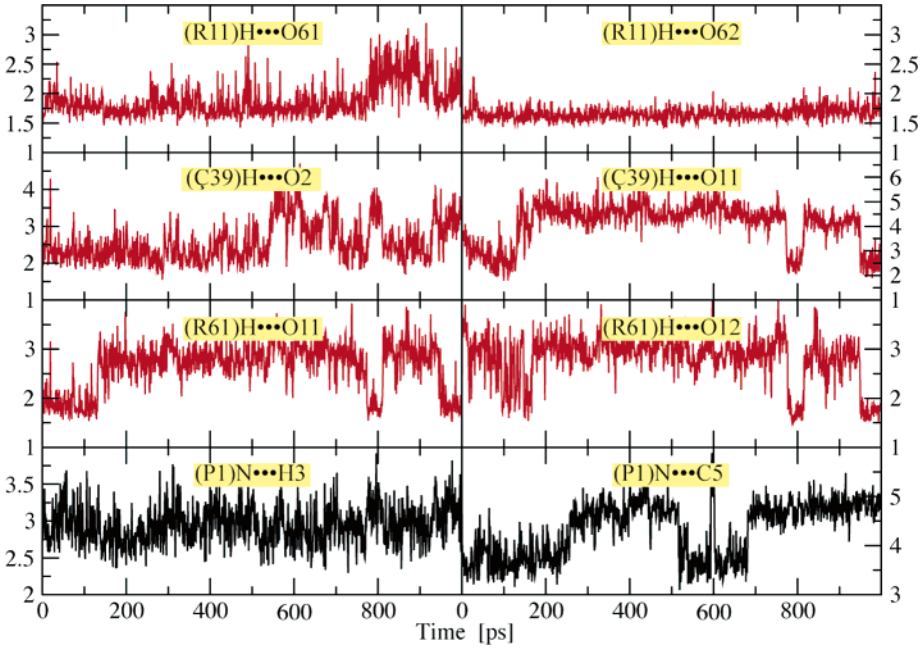

Figure 4. Trajectory of hydrogen bonds in the binding site for the **RÇR** system.

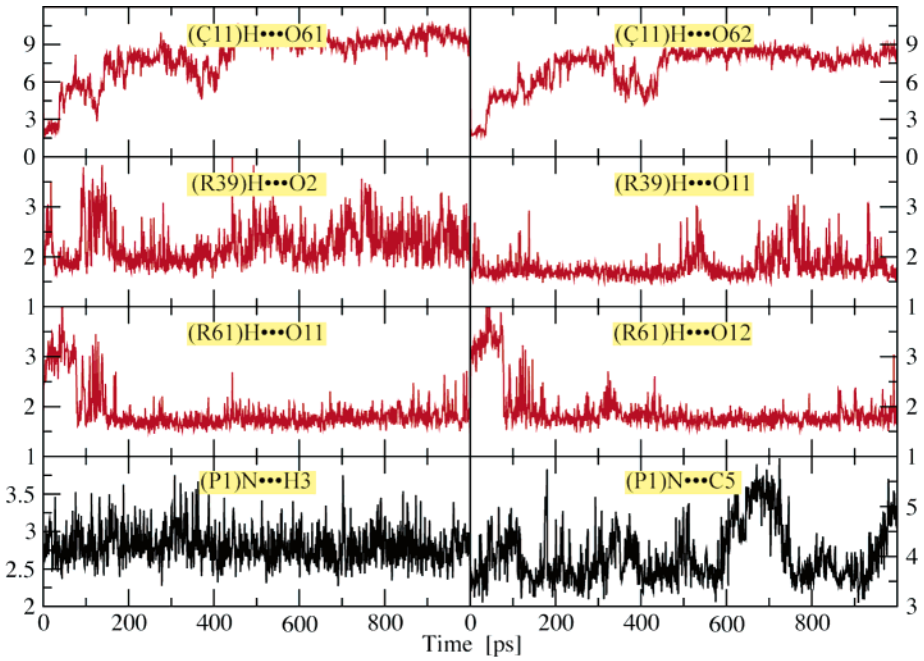

Figure 5. Trajectory of hydrogen bonds in the binding site for the **ÇRR** system.

TABLE 4: Hydrogen-Bond Descriptors of S1 in the ÇRR System

interaction	$\bar{r}$	$\bar{\tau}$	$\bar{r}_{-1}$	$\bar{\tau}_{-1}$	P
(**Ç11**)H−O61	2.25	11.7	8.32		0.03
(**Ç11**)H−O62	2.01	38.0	7.40		0.04
(**R39**)H−O2	2.13	10.9	3.08	1.58	0.87
(**R39**)H−O11	1.78	70.7	3.00	1.23	0.98
(**R61**)H−O11	1.79	4.8	3.12	5.20	0.93
(**R61**)H−O12	1.78	70.7	3.00	1.23	0.98
(**P1**)N−H3	2.64	2.3	3.02	1.9	0.55
(**P1**)N−C5			4.02	1001	

[a] See the text for definitions of symbols. Distances are given in angstroms. Times are given in picoseconds.

electrostatic stabilization at the 6-carboxylate end will most likely destabilize the intermediate. However, the magnitude of this effect is unlikely to be overwhelming.

During the MD run for **ÇRR**, the propensity of the substrate to change its conformation in the binding site, in the presence of the repulsive interaction with **Ç11′**, depends on the intramolecular parametrization of the substrate. As our parametrization of **S1** primarily aimed at reproducing the intermolecular interactions (see the Supporting Information for details), the ability of the substrate to undergo conformational changes may not be well reproduced. Thus, we performed QM/MM optimizations of selected snapshots from the reactant systems to investigate the **S1**−**P1** interaction at the QM level, where an appropriate description of conformational flexibility of the substrate is implicit.

QM/MM Optimization of Binding Sites. For selected snapshots (600, 700, 800, 900, and 1000 ps) the binding site of the wild-type enzyme and the three mutant systems were

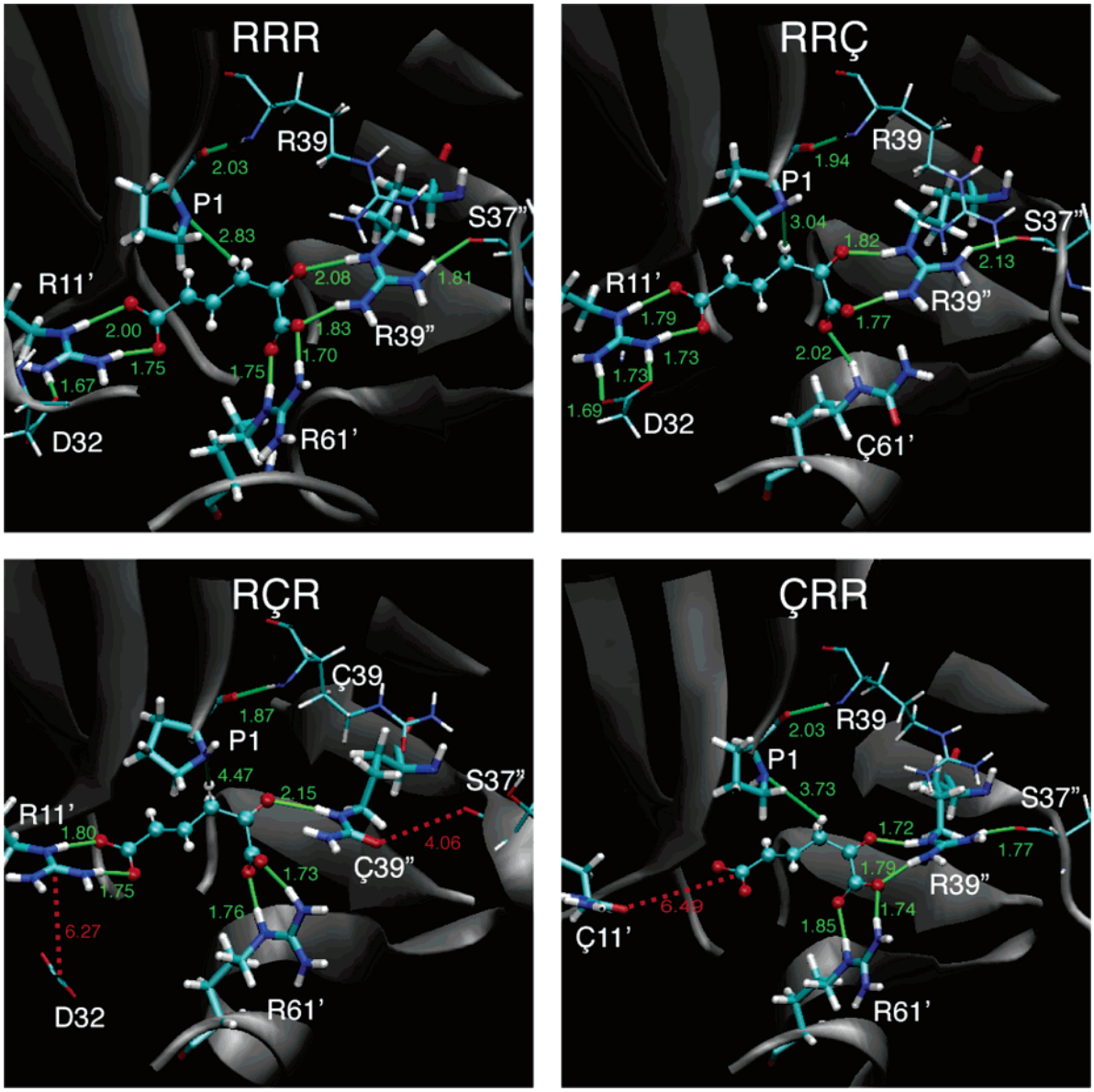

Figure 6. Representative snapshots for the binding sites of the wild-type and mutant systems optimized with BLYP/CHARMM (see text for details). Distances are given in angstroms.

optimized at the QM/MM level. A representative snapshot of each of the four systems is discussed below.

The **RRR** binding site clearly has a well-defined structure. The terminal proline residue forms a backbone hydrogen bond to the **R39** residue of the same monomer, which aids in orienting the residue in the binding site. Recently, the **R39** residue was suggested to play an *indirect* role in the binding of substrate.[58] Our calculations predict that the primary role of the remote **R39** residue is in stabilizing the position of **P1** through a backbone hydrogen bond between the two residues. In the inactive complex the position of **P1** is affected by the covalent binding to the inhibitor. This binding "pulls" the **R39** residue, through the backbone hydrogen bond, toward the active site. In the **RRR** complex, there is no evidence of a favorable "aromatic stacking" interaction between **R39** and **R39″** (the separation of C_ζ atoms is 4.74 Å) in the noncovalent binding of **S1**.

The **R11′** and **R39″** residues also form strong hydrogen bonds with neighboring residues (**D32** and **S37″**, respectively) that provide the general structure of the binding site in **RRR**. However, **R61′** has no strong stabilizing interactions with other residues in the enzyme, and thus, when no substrate is present, **R61′** is relatively free to alter its position. This observation is supported by X-ray studies of the unbound enzyme (PDB code 4OTA).[59] In these studies the position of **R61′** could not be resolved as a result of the flexibility of the residue in the absence of a substrate.

Despite the fact that **R61′** is not directly involved in defining the structure of the binding site, it plays an essential role in binding the 1-carboxylate terminus of the substrate. In the QM/MM optimization of **RRR** the two strong hydrogen bonds between **S1** and **R61′** remain intact. The interaction with **R39″** complements the **R61′** binding of the substrate, forming a second hydrogen bond (1.83 Å, **RRR**, Figure 6) to a 1-carboxylate O atom, in addition to binding the 2-carbonyl O of **S1** (2.08 Å). The strong hydrogen bond between **D32** and **R11′** (1.67 Å) positions the latter residue such that it is able to bind the 6-carboxylate terminus of **S1**. The interactions between **S1** and the arginine residues place one of the H atoms at C3 under the N atom of **P1** (2.83 Å), such that it can be abstracted to allow formation of the intermediate complex.

The Arg61Cit mutation has only a minor effect on the overall structure of the binding site. In the selected snapshot, one of

TABLE 5: Kinetic Parameters for the Isomerization of S1 by Wild-Type and Mutant 4-OT[15]

system	K_M (μM)	k_{cat} (s^{-1})	k_{cat}/K_M ($M^{-1}\ s^{-1}$)
RRR	62 ± 10	2500 ± 150	4.0×10^7
RRÇ	260 ± 25	1200 ± 70	4.5×10^6
RÇR	160 ± 40	1.5 ± 0.2	9.8×10^3
ÇRR	780 ± 120	24 ± 3	3.0×10^4
RÇÇ	nd	<0.5	nd
ÇRÇ	780 ± 270	5.4 ± 1.5	7.0×10^3
ÇÇR	nd	<0.5	nd
ÇÇÇ	nd	<0.5	nd

the hydrogen bonds between **Ç61′** and **S1** is broken, consistent with the flexible nature of the **Ç61′** residue deduced from the MD simulations of **RRÇ** ($P = 0.77$, Table 2). For compensation, the substrate binds more strongly to **R39″** (1.77, 1.82 Å, **RRÇ**, Figure 6), which results in a slight rotation of **S1** into the binding site and a corresponding shift in the position of **R39″**. This latter shift is reflected in the increase of the hydrogen-bond length between **R39″** and **S37″** (2.13 Å), relative to the **RRR** system. In addition, the movement of **S1** in the binding site slightly increases the distance between the abstractable proton and the N atom of **P1** (3.04 Å, RRÇ, Figure 6). However, these changes in the binding site structure and relative orientation of **S1** are minimal. The QM/MM optimizations thus confirm that the lack of dependence of the measured k_{cat} and K_M values (Table 5) on the mutation of Arg61 is due to the ability of **R39″** to compensate for the mutation rather than **R61′** playing a minimal role in binding the substrate, as previously suggested.[15,17]

In contrast to the Arg61Cit mutation, the Arg39Cit mutation has a pronounced effect on the structure of the binding site. To maintain the binding of the substrate the carbonyl group of **Ç39″** points out of the binding site of **RÇR**. However, this outward orientation results in lone-pair repulsion between the **Ç39″** carbonyl O atom and the backbone O atom of **S37″**. This interaction, which previously stabilized the binding site, causes **Ç39″** to be forced into the site, and **S1** is also pushed from its **RRR** position in a "knock-on" effect. The positioning of the abstractable H atom beneath the **P1** N atom is lost with the N···H distance being increased to 4.47 Å (**RÇR**, Figure 6). This change in the relative position of the substrate is expected to be the primary cause of the observed changes in the catalytic ability of the **RÇR** mutant (k_{cat} diminished by a factor of 1700 relative to **RRR**, Table 5).

The binding ability of the **RÇR** mutant is, however, only slightly affected (K_M increased by a factor of 4 relative to **RRR**, Table 5), again because of the flexibility of **R61′**. Despite the shift of **S1** in the binding site, **R61′** is able to adjust its position to maintain the strong hydrogen bonds (1.76, 1.73 Å, **RÇR**, Figure 6) observed in the parent system (1.75, 1.70 Å, **RRR**, Figure 6) without negatively affecting the binding site structure. The hydrogen bonds to **R11′** are also kept in the **RÇR** mutant, although at a further cost to the structure of the binding site. For **R11′** to maintain the hydrogen bonds to **S1** the residue must adjust its position in accordance with the shift initiated by the **Ç39″**−**S37″** repulsive interaction. The movement of **R11′** results in the loss of the strong hydrogen bonds between **D32** and **R11′**. Thus, we conclude that while the binding site is able to distort itself to maintain a strong binding of the substrate in the Arg39Cit mutation, this distortion leads to the loss of the catalytic ability of the enzyme. The dominant factor in this regard appears to be the inefficient positioning of **S1** in the mutant rather than the loss of electrostatic complementarity for the intermediate.

In the **ÇRR** system, the best orientation of the citrulline residue (i.e., resulting in the maximum number of hydrogen bonds for **S1**) has the carbonyl group of **Ç11′** directed into the binding site (**ÇRR**, Figure 6), which results in repulsion between the 6-carboxylate group of **S1** and **Ç11′** ((**Ç11′**)O−C6(**S1**) = 6.49 Å) and stronger binding interactions at the 1-carboxylate end of the substrate, as observed in the MD simulation. The repulsion between the 6-carboxylate end and **Ç11′** is reflected in the experimental K_M value of the **ÇRR** mutant, which is increased 13-fold relative to **RRR** (Table 5). Nonetheless, the strong hydrogen bonds between **R39″** and **S1** are maintained as well as the stabilizing interaction between **R39″** and **S37″**. Furthermore, the 1-carboxylate group also maintains the strong hydrogen bonds with **R61′**, which are present in the parent system. Thus, unlike the **RÇR** case, only half of the binding site is distorted in the **ÇRR** mutant when the substrate is present. This partial distortion still allows the mutant to bind the substrate despite the complete loss of stabilizing interactions with residue 11. Similarly to the **RÇR** system, there is a shift of **S1**, which is primarily an internal rotation that yields an increase in the (**S1**)H···N(**P1**) distance to 3.73 Å (**ÇRR**, Figure 6) and thus diminishes the catalytic ability of the **ÇRR** mutant (k_{cat} decreased by 105-fold relative to **RRR**, Table 5).

Analogues with Multiple Mutations. In addition to the single mutation studies described above, we have also carried out analogous studies for systems with more than one mutation (i.e., **RÇÇ**, **ÇRÇ**, **ÇÇR**, and **ÇÇÇ**). Experimentally, the catalytic activity of these analogues was undetected in all cases, except the **ÇRÇ** analogue (Table 5). The observation that mutations of residue 11 and/or residue 39 result in distortions of the binding site also holds true in the case of multiple mutations. The MD simulations of these analogues indicate further disruption of the binding site structures, and consequently the positioning of the abstractable H atom is compromised. The exception to this trend is the **ÇRÇ** analogue, which is understood by the cooperativity of residues 61 and 39 in binding the substrate and the flexibility of residue 61. Residue **Ç61′** orients itself to allow a binding interaction with **S1** similar to that obtained by **R61′** such that the **ÇRÇ** analogue differs only slightly with respect to the **ÇRR** analogue, which is observed experimentally. Details of the optimized binding sites for the multiple mutant structures are available in the Supporting Information.

Conclusions

Although the kinetic parameters k_{cat} and K_M have not been calculated explicitly in this work, the combined MM−MD and QM/MM study of the 4-OT enzyme and its mutant analogues provides several new insights into the experimental observations of the catalytic and binding abilities of these systems. (1) **R61′** is a flexible residue that complements **R39″** in binding the 1-carboxylate terminus of the substrate. (2) The Arg61Cit mutation has only a minor effect on the binding and catalytic ability of the enzyme due to the ability of **Ç61′** to maintain the binding of the substrate without distorting the binding site. (3) The Arg39Cit mutation causes a disruption of the binding site due to the repulsive interaction between the side-chain O atom of **Ç39″** and the backbone O atom of **S37″**. (4) The disruption of the binding site structure is most likely the primary cause of the loss of catalytic ability in the **RÇR** system. (5) The binding ability in the **RÇR** system is only partially affected by the mutation due to the ability of **R61′** to complement the binding of the 1-carboxylate terminus of **S1**. (6) The loss of the catalytic ability in the **ÇRR** system is primarily caused by the disruption

SCHEME 5: Revised Scheme of the Binding Site of 4-OT

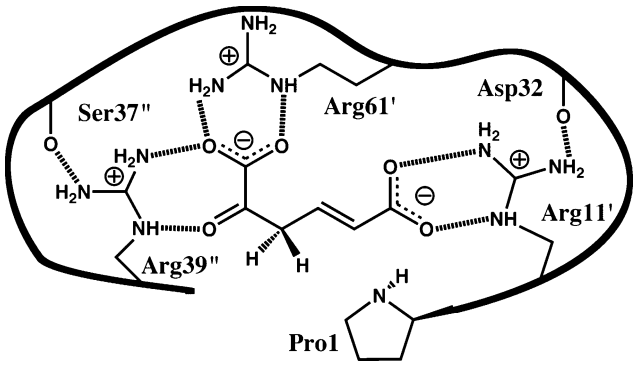

of the binding site that results from the repulsion between the side-chain O atom of **Ç11′** and the 6-carboxylate terminus of **S1**. (7) The binding ability of the **ÇRR** mutant is also decreased by this repulsive interaction. (8) The role of the remote **R39** residue is to stabilize the position of **P1** through a backbone hydrogen bond between the two residues.

Taken together, these results indicate that the primary role of the arginine residues in the binding site is to position the substrate for the proton abstraction reaction. The mutation of residues **R11′** and **R39″** leads to a distortion of the binding site and a change in the positioning of the substrate. Previous explanations for the observed changes in k_{cat} and K_M upon mutation, in terms of electrostatic complementarity,[15] were based on a static picture of the binding site that neglects the changes arising from interactions with surrounding residues, in particular **S37″** and **D32′**. The present computational results indicate that the picture of the 4-OT binding site needs to be extended to include these residues, as shown in Scheme 5.

This report also highlights two methodological issues that arise in the study of these systems. (A) The use of hydrogen-bond descriptors provides a quantitative overview of the stability of a binding site during an MD simulation. The parametrization of the substrate is sufficient for describing the intermolecular interactions between the substrate and the binding site residues. (B) In the cases where the substrate has a larger degree of flexibility in the binding site, optimization at the QM/MM level is advisable to take such effects into account without relying on the force field parametrization. The QM/MM optimization of the reactant systems leads to a better understanding of the factors underlying the experimentally observed changes in k_{cat} and K_M.

Acknowledgment. This work was supported by the DIP program (Grant No. DIP-F.6.2).

Supporting Information Available: Extensive material describing the setup and preparation of the different mutants as well as details of the MD simulations and QM/MM geometry optimizations and the final optimized structures in PDB format. This material is available free of charge via the Internet at http://pubs.acs.org.

References and Notes

(1) Harris, J. L.; Craik, C. S. *Curr. Opin. Chem. Biol.* **1998**, *2*, 127.
(2) Metanis, N.; Keinan, E.; Dawson, P. E. *J. Am. Chem. Soc.* **2005**, *127*, 5862.
(3) *Protein Engineering*; Oxender, D. L., Fox, C. F., Eds.; Alan R. Liss: New York, 1987.
(4) Pick, L.; Hurwitz, J. *J. Biol. Chem.* **1986**, *261*, 6684.
(5) Douthwaite, J.; Jermutus, L. *Curr. Opin. Drug Discovery Dev.* **2006**, *9*, 269.
(6) Hoogenboom, H. R. *Nature Biotechnol.* **2005**, *23*, 1105.
(7) Reetz, M. T. *Angew. Chem., Int. Ed.* **2001**, *40*, 284.
(8) Reetz, M. T.; Bocola, M.; Carballeira, J. D.; Zha, D. X.; Vogel, A. *Angew. Chem., Int. Ed.* **2005**, *44*, 4192.
(9) Tann, C. M.; Qi, D. F.; Distefano, M. D. *Curr. Opin. Chem. Biol.* **2001**, *5*, 696.
(10) Zoller, M. J.; Smith, M. *Methods Enzymol.* **1987**, *154*, 329.
(11) Harayama, S.; Rekik, M.; Ngai, K. L.; Ornston, L. N. *J. Bacteriol.* **1989**, *171*, 6251.
(12) Whitman, C. P. *Arch. Biochem. Biophys.* **2002**, *402*, 1.
(13) Fitzgerald, M. C.; Chernushevich, I.; Standing, K. G.; Kent, S. B. H.; Whitman, C. P. *J. Am. Chem. Soc.* **1995**, *117*, 11075.
(14) Fitzgerald, M. C.; Chernushevich, I.; Standing, K. G.; Whitman, C. P.; Kent, S. B. H. *Proc. Natl. Acad. Sci. U.S.A.* **1996**, *93*, 6851.
(15) Metanis, N.; Brik, A.; Dawson, P. E.; Keinan, E. *J. Am. Chem. Soc.* **2004**, *126*, 12726.
(16) Taylor, A. B.; Czerwinski, R. M.; Johnson, W. H.; Whitman, C. P.; Hackert, M. L. *Biochemistry* **1998**, *37*, 14692.
(17) Harris, T. K.; Czerwinski, R. M.; Johnson, W. H.; Legler, P. M.; Abeygunawardana, C.; Massiah, M. A.; Stivers, J. T.; Whitman, C. P.; Mildvan, A. S. *Biochemistry* **1999**, *38*, 12343.
(18) Miller, B. G.; Wolfenden, R. *Annu. Rev. Biochem.* **2002**, *71*, 847.
(19) Zhang, X. Y.; Houk, K. N. *Acc. Chem. Res.* **2005**, *38*, 379.
(20) Chen, L. H.; Kenyon, G. L.; Curtin, F.; Harayama, S.; Bembenek, M. E.; Hajipour, G.; Whitman, C. P. *J. Biol. Chem.* **1992**, *267*, 17716.
(21) Lian, H. L.; Whitman, C. P. *J. Am. Chem. Soc.* **1993**, *115*, 7978.
(22) Whitman, C. P.; Aird, B. A.; Gillespie, W. R.; Stolowich, N. J. *J. Am. Chem. Soc.* **1991**, *113*, 3154.
(23) Cisneros, G. A.; Liu, H. Y.; Zhang, Y. K.; Yang, W. T. *J. Am. Chem. Soc.* **2003**, *125*, 10384.
(24) Czerwinski, R. M.; Harris, T. K.; Johnson, W. H.; Legler, P. M.; Stivers, J. T.; Mildvan, A. S.; Whitman, C. P. *Biochemistry* **1999**, *38*, 12358.
(25) Johnson, W. H.; Czerwinski, R. M.; Fitzgerald, M. C.; Whitman, C. P. *Biochemistry* **1997**, *36*, 15724.
(26) *SYBYL*, version 6.9; Tripos, Inc.: St. Louis, MO, 2004.
(27) Word, J. M. *Reduce*, version 2.21; Biochemistry Department, Duke University: Durham, NC, 2003.
(28) Word, J. M.; Lovell, S. C.; Richardson, J. S.; Richardson, D. C. *J. Mol. Biol.* **1999**, *285*, 1735.
(29) Soares, T. A.; Goodsell, D. S.; Briggs, J. M.; Ferreira, R.; Olson, A. J. *Biopolymers* **1999**, *50*, 319.
(30) Li, H.; Robertson, A. D.; Jensen, J. H. *Proteins: Struct., Funct., Bioinf.* **2005**, *61*, 704.
(31) *CHARMM*, version c31b1; Department of Chemistry and Chemical Biology, Harvard University: Cambridge, MA, 2004.
(32) Brooks, B. R.; Bruccoleri, R. E.; Olafson, B. D.; States, D. J.; Swaminathan, S.; Karplus, M. *J. Comput. Chem.* **1983**, *4*, 187.
(33) MacKerell, A. D.; Brooks, B. R.; Brooks, C. L., III.; Nilsson, L.; Roux, B.; Won, Y.; Karplus, M. In *Encyclopedia of Computational Chemistry*; Schleyer, P. v. R., Ed.; Wiley: Chichester, U. K., 1998; Vol. 1, p 271.
(34) Foloppe, N.; MacKerell, A. D. *J. Comput. Chem.* **2000**, *21*, 86.
(35) MacKerell, A. D.; Banavali, N. K. *J. Comput. Chem.* **2000**, *21*, 105.
(36) MacKerell, A. D., Jr.; Bashford, D.; Bellott, R. L.; Dunbrack, R. L., Jr.; Evanseck, J. D.; Field, M. J.; Fischer, S.; Gao, J.; Guo, H.; Ha, S.; Joseph-McCarthy, D.; Kuchnir, L.; Kuczera, K.; Lau, F. T. K.; Mattos, C.; Michnick, S.; Ngo, T.; Nguyen, D. T.; Prodhom, B.; Reiher, W. E., III.; Roux, B.; Schlenkrich, M.; Smith, J. C.; Stote, R.; Straub, J.; Watanabe, M.; Wiorkiewicz-Kuczera, J.; Yin, D.; Karplus, M. *J. Phys. Chem. B* **1998**, *102*, 3586.
(37) The vdW parameters in CHARMM are quite robust. Thus, these parameters were taken from similar atoms existing in the standard force field.
(38) Overlapping is defined by the distance between the TIP3P oxygen atom and any non-TIP3P heavy atom: $R(O-X)$. If $R(O-X) < 2.8$ Å, then the TIP3P water is deleted.
(39) Brooks, C. L.; Karplus, M. *J. Chem. Phys.* **1983**, *79*, 6312.
(40) Dewar, M. J. S.; Zoebisch, E. G.; Healy, E. F.; Stewart, J. J. P. *J. Am. Chem. Soc.* **1985**, *107*, 3902.
(41) Becke, A. D. *Phys. Rev. A* **1988**, *38*, 3098.
(42) Lee, C. T.; Yang, W. T.; Parr, R. G. *Phys. Rev. B* **1988**, *37*, 785.
(43) Schäfer, A.; Huber, C.; Ahlrichs, R. *J. Chem. Phys.* **1994**, *100*, 5829.
(44) *ChemShell*, version 3.0a3; CCLRC Daresbury Laboratory: Cheshire, U.K., 2004.
(45) Sherwood, P.; de Vries, A. H.; Guest, M. F.; Schreckenbach, G.; Catlow, C. R. A.; French, S. A.; Sokol, A. A.; Bromley, S. T.; Thiel, W.; Turner, A. J.; Billeter, S.; Terstegen, F.; Thiel, S.; Kendrick, J.; Rogers, S. C.; Casci, J.; Watson, M.; King, F.; Karlsen, E.; Sjøvoll, M.; Fahmi, A.; Schäfer, A.; Lennartz, C. *J. Mol. Struct. (THEOCHEM)* **2003**, *632*, 1.

(46) Thiel, W. *MNDO99*, version 6.1; Max-Planck-Institut für Kohlenforschung: Mülheim an der Ruhr, Germany, 2004
(47) *TURBOMOLE*, version 5.7.1; COSMOlogic GmbH & Co. KG: Leverkusen, Germany, 2004.
(48) Ahlrichs, R.; Bär, M.; Häser, M.; Horn, H.; Kölmel, C. *Chem. Phys. Lett.* **1989**, *162*, 165.
(49) Häser, M.; Ahlrichs, R. *J. Comput. Chem.* **1989**, *10*, 104.
(50) Horn, H.; Weiss, H.; Häser, M.; Ehrig, M.; Ahlrichs, R. *J. Comput. Chem.* **1991**, *12*, 1058.
(51) Treutler, O.; Ahlrichs, R. *J. Chem. Phys.* **1995**, *102*, 346.
(52) de Vries, A. H.; Sherwood, P.; Collins, S. J.; Rigby, A. M.; Rigutto, M.; Kramer, G. J. *J. Phys. Chem. B* **1999**, *103*, 6133.
(53) Lin, H.; Truhlar, D. G. *J. Phys. Chem. A* **2005**, *109*, 3991.
(54) Lin, H.; Truhlar, D. G. *Theor. Chem. Acc.*, published online July 8, http://dx.doi.org/10.1007/s00214-006-0143-z.
(55) Billeter, S. R.; Turner, A. J.; Thiel, W. *Phys. Chem. Chem. Phys.* **2000**, *2*, 2177.
(56) Harris, T. K.; Legler, P. M.; Czerwinski, R. M.; Abeygunawardana, C.; Massiah, M. A.; Stivers, J. T.; Whitman, C. P.; Mildvan, A. S. *Biophys. J.* **1999**, *76*, A178.
(57) Subramanya, H. S.; Roper, D. I.; Dauter, Z.; Dodson, E. J.; Davies, G. J.; Wilson, K. S.; Wigley, D. B. *Biochemistry* **1996**, *35*, 792.
(58) Azurmendi, H. F.; Miller, S. G.; Whitman, C. P.; Mildvan, A. S. *Biochemistry* **2005**, *44*, 7725.
(59) Taylor, A. B. Ph.D. Thesis, University of Texas at Austin, Austin, TX, 1998.